Finite-Element Analysis of Optical and Microwave Waveguide Problems

B. M. AZIZUR RAHMAN, MEMBER, IEEE, AND J. BRIAN DAVIES, MEMBER, IEEE

Abstract —**A vector *H*-field formulation is developed for electromagnetic wave propagation for a wide range of guided-wave problems. It is capable of solving microwave or optical waveguide problems with arbitrarily anisotropic materials. We have introduced infinite elements to extend the region of explicit field representation to infinity, to consider open-type waveguides more accurately. Computed results are given for a variety of optical planar guides, image lines, and waveguides containing skew anisotropic dielectric.**

I. Introduction

As THE RANGE of guiding structures becomes more intricate, so the need for computer analysis becomes greater and more demanding. Some guides are so important as to justify specialized techniques adapted to their needs, such as microstrip or the various optical fibers. But, for its flexibility or versatility, the finite-element method has become a powerful tool throughout engineering.

In this work, we are concerned with guiding structures that are uniform in the direction of wave propagation, but where the "guiding" arises from nonuniformity of material in the transverse dimensions. Any guide cross section can be divided into a patchwork of triangular elements, and the appropriate field components represented by polynomials over these elements. For open-type guides, beyond the cross section represented by these orthodox triangular elements, we add "infinite elements"—rectangular strips which give explicit field representations to infinity in all of the necessary transverse directions. This is shown in Fig. 1 for a channel waveguide, where, because of the mirror symmetry, the problem is reduced to a half.

The finite-element variational formulation is made via a full $\boldsymbol{H}$ vector field [1], where each field component H_x, H_y, and H_z is separately represented by a function continuous over the whole transverse plane. This is particularly convenient for guides with permittivity discontinuities (e.g., image guide) where continuity of $\boldsymbol{H}$-field components is automatically satisfied.

Each element may have a different dielectric constant, and the constant may be arbitrarily tensor (loss-free). Applying stationariness of the variational form reduces the problem to a standard eigenvalue matrix equation. For a large-order matrix, most of the terms are zero, and so we have used a truly sparse method [2] to solve the equation.

Manuscript received January 5, 1983; revised August 4, 1983.
The authors are with the Department of Electronic and Electrical Engineering, University College London, London WC1E 7JE.

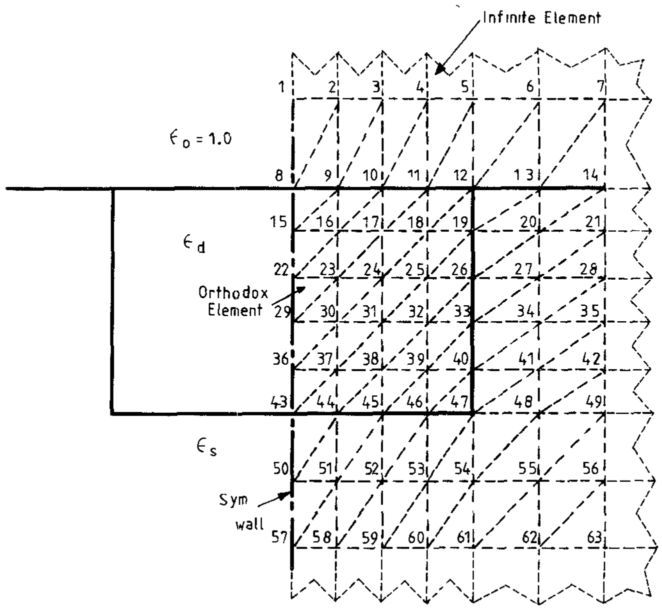

Fig. 1. Node representation of a channel guide, with orthodox and infinite elements.

II. Variational Formulation for Finite Elements

There are different forms of variational formulation used for finite-element methods. The scalar form of finite-element method has been used for solving homogeneous waveguide problems [3], [4]. This single scalar formulation is inadequate for the inherently hybrid mode situation of inhomogeneous or anisotropic problems. A finite-element formulation using an axial component of the fields (E_z and H_z) has been used to solve many different types of guiding structures problems [5]–[9]. This formulation cannot, without destroying the canonical form of the eigenvalue matrix, treat general anisotropic problems. For a waveguide with arbitrary dielectric distribution, the satisfying of boundary conditions in this method can be quite difficult. Another fundamental disadvantage of this method for optical dielectric waveguide problems is that it considers axial components of the fields, which are the least important components of the six-vector field. Berk [1] derived vector variational formulations in the form of a Rayleigh quotient for loss-free anisotropic waveguides and resonators. Later, Morishita and Kumagai [10] derived similar vector variational formulations. By contrast, a vector $\boldsymbol{E}$ field was applied by English and Young [11]. This formula-

0018-9480/84/0100-0020$01.00

tion can solve general anisotropic problems. They considered a vector $\boldsymbol{E}$ formulation as it involved more Dirichlet (rather than Neumann) boundary conditions associated with the fields. But for this formulation, the natural boundary condition is that of a magnetic wall, which cannot be left free for an electric wall boundary. As the necessary boundary condition $\boldsymbol{n} \times \boldsymbol{E} = 0$ must be imposed on any conducting boundaries, it is an added difficulty to implement that boundary condition on arbitrarily shaped guide walls. Another disadvantage of this formulation is that at the dielectric interface it needs special consideration to ensure continuity of the tangential components of the fields. Ohtaka *et al.* [12] used a variational form in terms of the transverse component of $\boldsymbol{H}$; compared with the full three-vector $\boldsymbol{H}$, this involves additional differentiation which would be particularly disadvantageous with a finite element approach. For many purposes, a vector $\boldsymbol{H}$-field formulation [13] has the advantage over all others. In this formulation, the natural boundary condition is that of an electric wall, so that for arbitrary conducting guide walls it can be left free. In this formulation, the chosen field is continuous at the dielectric interfaces, and so it is very convenient for the finite-element solution of dielectric waveguide problems. In this formulation, we can also consider general anisotropic problems, which are important for many active and passive integrated optics structures.

This vector $\boldsymbol{H}$-field formulation can be written as [1]

$$\omega^2 = \frac{\int (\text{Curl}\,\boldsymbol{H})^* \cdot \epsilon^{-1} \cdot \text{Curl}\,\boldsymbol{H}\,dV}{\int \boldsymbol{H}^* \cdot \hat{\mu} \cdot \boldsymbol{H}\,dV} \tag{1}$$

where $\hat{\epsilon}$ and $\hat{\mu}$ can be general anisotropic permittivity and permeability of the loss-free medium, respectively. As the natural boundary condition is that of an electric wall, we need not force any boundary condition on conducting guide walls. But for regularly shaped waveguides, and at the symmetric walls (if applicable), we can enforce the boundary conditions to reduce the problem size.

III. Finite-Element Formulation

In the finite-element method [14], we first discretize the entire problem domain into a finite number of triangular subregions, called elements. In general, using many elements, we can approximate any continuum with a complex boundary and with an arbitrary index distribution to such a degree that an accurate analysis can be carried out. The field functions (each of H_x, H_y, and H_z) are defined by a set of algebraic polynomials over each element in the transverse plane, and longitudinal dependence $\exp(-j\beta z)$ is assumed, for given β. By expressing these fields in terms of "nodal values," most or all of which occur on the element boundaries, the resulting field components can be continuous over the whole domain. The extremum functional from (1) is then minimized with respect to the nodal values of the field components. In this way, the minimization generates a set of linear algebraic eigenvalue equations. This eigenvalue equation can be written as

$$Ax - \lambda Bx = 0 \tag{2}$$

where A is a complex hermitian, B is a real symmetric matrix, and λ is proportional to ω^2. We can solve this eigenvalue problem by one of various standard subroutines to get different eigenvectors and eigenvalues.

In general, the matrices A and B are quite sparse and have the same sparsity pattern. In the finite-element method, we discretize the whole problem domain in many smaller triangles, so that the continuous field problem is reduced to finding fields at discrete nodes, where the unknown field value is only coupled to the field values of the neighboring nodes. When we divide the problem domain into many regularly shaped triangles, then the number of nonzero terms per row and/or per column in A or B matrices will be a maximum of seven, irrespective of the order of the matrices (for scalar field formulation with first-order "shape functions," viz. first-degree polynomials). The nonzero coefficients can be even lower than seven per row or column when we consider nodal points on, or adjacent to, the boundary. Their coupling increases when we use higher order shape functions or more field components per nodal points, but always a very high proportion of the A and B matrix elements are zero. As an example, if we take a typical problem, using vector $\boldsymbol{H}$ field and a first-order shape function, when the order of the matrices is 397, then the percentage of nonzero terms is only 4.69 percent. We have exploited geometric symmetry and applied required boundary conditions at the time of assembling the global matrices, so reducing the storage required, as only the nonzero elements of the reduced matrices have been stored. Using a "search-limiting algorithm," we have greatly reduced the searching time required to decide whether a particular contribution to the global matrix has been made earlier or not.

In contrast to the usual dense and band-matrix algorithms [15], we have used a specially developed [16] "arbitrary sparse matrix" algorithm. Like the "subspace iteration" and "Sturm count" algorithms described by Bathe and Wilson [15], any band of adjacent eigenvalues can be safely computed, together with their associated eigenvectors. The advantage of the sparse matrix version is in taking into account all of the many zeros of (2), and so allowing a larger matrix order for given computer store. Its storage requirement is roughly proportional to the order of the matrices, rather than the square of the order of matrices, as in the dense version. This subroutine can find one or any number of eigenvalues (along with their eigenvectors) close to a specified point in the spectrum.

One question of tradeoffs in finite elements is (for given computer store and/or computer time) whether to use low-degree polynomials in many elements or high-degree polynomials in few elements. The "correct" choice, for most accurate results, depends on the application and on the matrix algorithm used to solve (2). For any arbitrarily shaped waveguide with arbitrary index distribution, our experience is that better accuracy is achieved (for given computer time and storage) by using many small-order triangles rather than fewer higher order triangles. The lower order shape function can represent the problem domain more accurately for a given order of matrix eigenvalue problem and gives higher sparsity of the matrices, and so it is advantageous when (as in our case) a completely sparse algorithm is used to solve the matrix eigenvalue problems. For all our modeling of 1) optical stripe guides with smooth refractive profiles, 2) image guides with a rather irregularly shaped cross section, and 3) guides with skew anisotropic permittivity (all illustrated later in this paper), the first-degree polynomial has been used and has proved to be effective.

IV. Infinite Elements

One property of the open-type waveguide is that finite fields exist in the region outside the guide. Outside the guide core, the field decays and the region of interest extends to infinity. The modeling of the infinite transverse extent of the waveguide presents a problem, and in orthodox finite-element discretization [3]–[9] one does not extend the region of consideration up to infinity. This extension of the problem domain is particularly important for the solutions close to cutoff, as (by definition of cutoff) the fields decay slowly and the region of significant field value can be arbitrarily large. To date, the customary approach is the simple truncation, which sets artificial boundary walls enclosing the guide [9]. In this case, care has to be taken so that it is sufficiently remote for the influence of the position of this artificial wall to be negligible, and at the same time it is sufficiently close to limit the necessary number of finite elements. One technique [8] involves shifting the virtual boundary wall to satisfy a given criterion for the maximum field strength at that wall.

Another approach is to use a recursion technique [17] to generate the matrix representing the region outside the main domain. It is possible to find the internal and external solutions and to match them on an imaginary boundary, some sort of integral solution being possible for the outside region. McDonald and Wexler [18] have used the finite-element method for a bounded region along with an integral equation for an unbounded region. In field matching techniques, these "two region solutions" are quite common [19].

Boundary elements have been used by Yeh *et al.* [20], considering an exponential decay outside the guide core. But in their method, because of nonconformity of the two coordinate systems, the fields used were not continuous. Bettes [21] has used infinite elements with a Cartesian coordinate system, using an exponential decay and Lagrange multipliers, for fluid flow problems.

An infinite element is a finite element that indeed extends to infinity, and shape functions for such an element should be realistic to represent the fields and should be square integrable over an infinite-element area, to satisfy the radiation condition [22]. For an infinite element extending towards infinity in the x-direction, we can assume exponential decay in x and conventional shape function

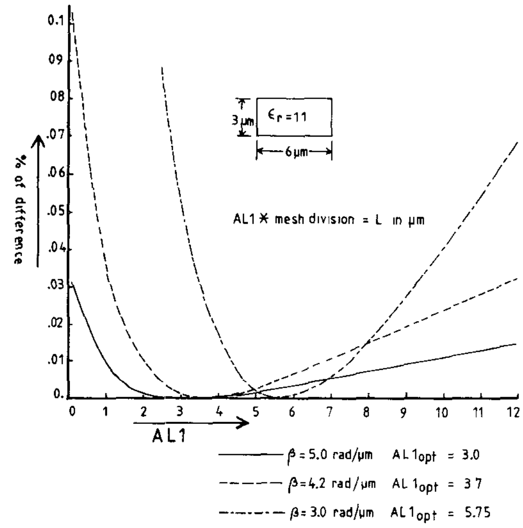

Fig. 2. Optimization of a decay parameter at three different frequencies.

dependence in the y-direction. It can be written as

$$N_i(x, y) = f_i(y)\exp(-x/L) \tag{3}$$

where L is a decay length. Similarly, we can have infinite elements extending towards the y-direction by considering exponential decay in y. Similarly, by assuming exponential decay in both x and y, we can consider a rectangular or quadrant element extending towards infinity in both x- and y-directions. Integration of these shape functions or their derivatives over the infinite elements are finite, and can be simply carried out. Combining all of these elements along with the conventional finite element, we can represent any open-type waveguide cross-sectional domain very conveniently, with each field component being continuous over the whole infinite domain.

Fig. 1 illustrates the use of infinite elements for the analysis of a "channel" guide [23]. Orthodox triangular elements are used in the central region. The infinite elements can be seen extending in all Cartesian directions. In infinite elements we need to assume exponential decay factors, which are unknown at the beginning. The best value of decay parameter depends not only on the specific problem, but also on the operating frequency, and can also be different for different elements. Nevertheless, we would contend that any reasonable parameter will be better than considering a perfect reflector at the same boundary location. Instead of assuming many decay parameters, we restrict ourselves to a few, and subsequently optimize them. Varying any one of them, we can find a stationary solution, and the value of the parameter which makes the solution stationary is taken as the optimized value. In Fig. 2, we show the stationary nature of the solution for ω^2 as ordinate with variation of a particular decaying factor $AL1$ for three different propagation constants (i.e., for three frequencies). In Fig. 3, we show the variation of optimized $AL1$ with a propagation constant. We observe that as the frequency increases, the $AL1_{\text{opt}}$ is reduced, which corresponds to the fact that fields are more confined inside the guide at the

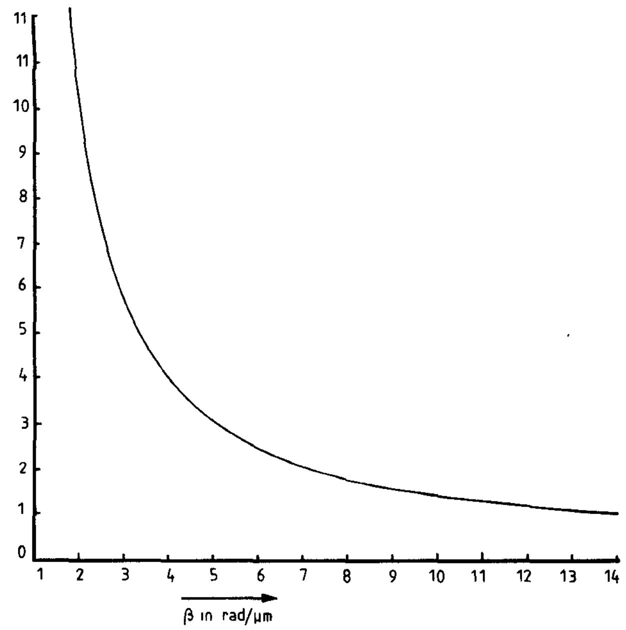

Fig. 3. Variation of an optimized decay parameter with propagation constants.

higher frequencies. Figs. 2 and 3 are for a rectangular dielectric waveguide with dimension 6.0 μm $\times$ 3.0 μm having $\epsilon_r = 1.1$.

V. Spurious Modes

Like other workers [2], [6], [8], [9], and [13], we have observed the presence of spurious solutions along with the physical solutions. These spurious solutions apparently exist for all types of vector formulations. Their exact cause of appearance still is not resolved. It could be due to various factors such as enforcement of boundary conditions, the positive definiteness of the operator, possibly due to the nonzero divergence of the trial fields, or maybe because the system is too flexible [24]. They can be identified from the true solutions by different ways, one of which is by inspecting corresponding eigenvectors. We have developed a procedure which gives a very easy identification of the probability of being a physical or spurious solution. The logic behind the scheme is the fact that a physical eigenvector should obey $\operatorname{div} \boldsymbol{B} = 0$. Thus we calculate $\operatorname{div} \boldsymbol{H}$ for each eigenvector of interest and compare their values. We have observed that, for all problems, a true solution has lower $\operatorname{div} \boldsymbol{H}$ than the spurious solutions. Comparing the $\operatorname{div} \boldsymbol{H}$ value of a particular mode with others helps in identifying their validity. In all these cases, we have calculated $\operatorname{div} \boldsymbol{H}$ from the discrete nodal field values obtained after the solution of the eigenvalue equation (2).

VI. Rectangular Dielectric Waveguides

A dielectric fiber with a refractive index higher than its surrounding region is a simple form of an optical waveguide. These guides support various hybrid modes, which can be grouped into two families H^x_{mn} and H^y_{mn}, and we have used the mode designation as used by Marcatili [23]. We show propagation characteristics for H^x_{11} and H^x_{31}

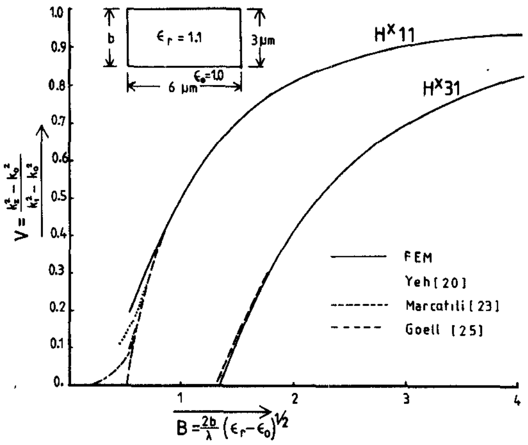

Fig. 4. Propagation characteristics for a rectangular dielectric waveguide, finite element divisions 8 $\times$ 8 (128 triangles).

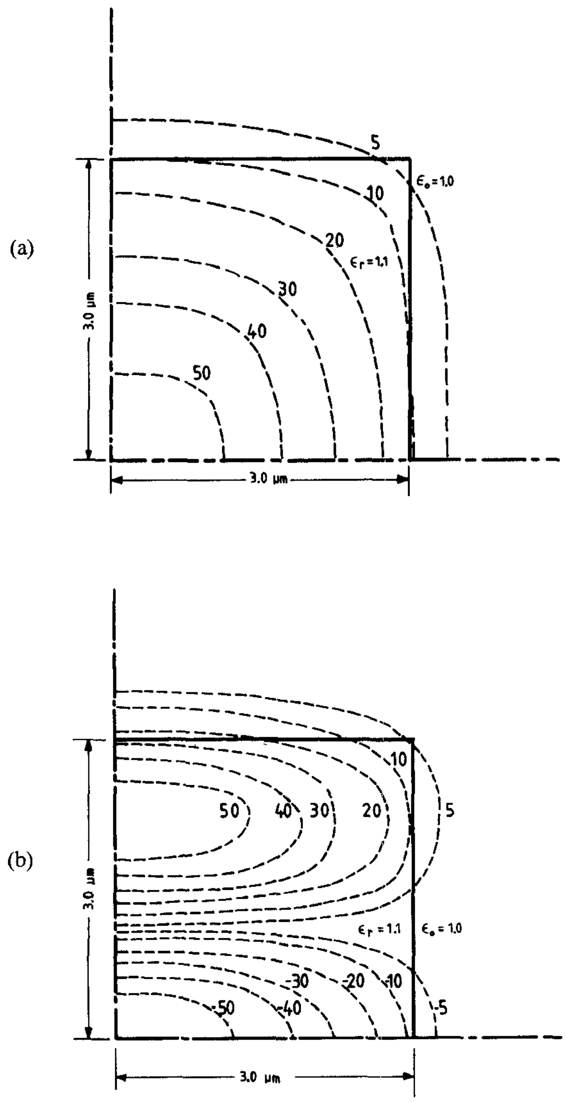

Fig. 5. H_x field contour in a rectangular dielectric waveguide. (a) H^x_{11} mode. (b) H^x_{13} mode.

modes, for guide dimension 6.0 μm $\times$ 3.0 μm and $\epsilon_r = 1.1$ in Fig. 4, including a comparison with Yeh [20], Marcatili [23], and Goell [25]. Fig. 5(a) and (b) shows the eigenvec-

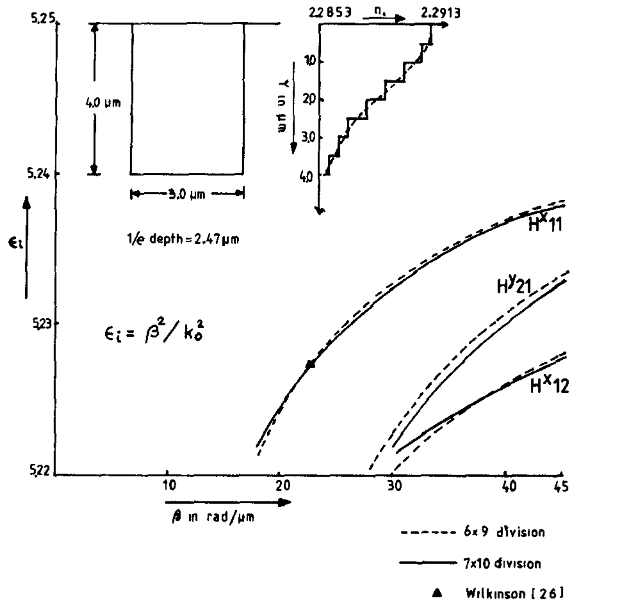

Fig. 6. Propagation characteristics of a titanium-diffused channel waveguide with a refractive index varying as a Gaussian function.

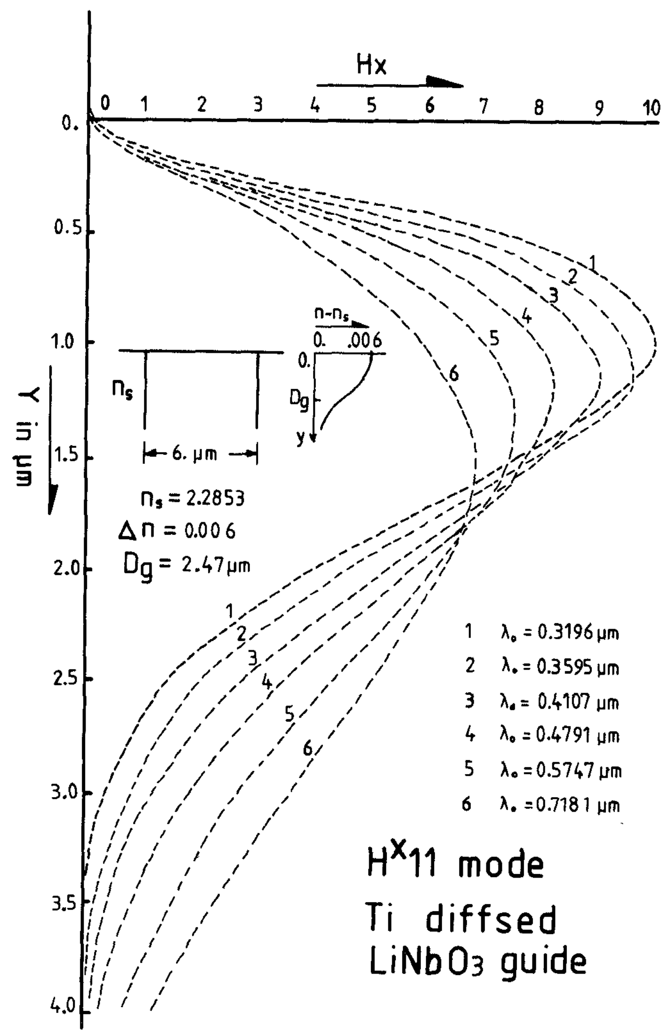

Fig. 7. Field distribution with depth y for titanium-diffused channel waveguide at different wavelengths.

tors for the H_{11}^x mode and the H_{13}^x mode, respectively, for a guide dimension of 6.0 μm $\times$ 6.0 μm with $\epsilon_r = 1.1$.

VII. Channel Waveguide

A channel, or embedded-strip, waveguide is a special waveguide of practical interest. The guide can be fabricated with more relaxed requirements for the resolution and edge roughness than for the rectangular dielectric waveguide. The refractive index of the guiding section is higher than that of the substrate, and this difference can be achieved in just one step, or smoothly, such as a linear or exponential variation. For comparison with the experiment, we have solved a titanium-diffused channel waveguide, with a strip width of 3.0 μm and with a refractive index following a Gaussian function of guide depth. At the top of the guide, the refractive index is 2.2913 and that of the substrate is 2.2853. At the depth of 2.47 μm, it attains the value $2.2853 + (2.2913 - 2.2853)/e$. Propagation characteristics were computed for the H_{11}^x, H_{21}^y, and H_{12}^x modes, and the results are shown in Fig. 6. It shows good agreement with the point obtained experimentally by Wilkinson [26]. The field variation with guide depths for different frequencies is shown in Fig. 7.

VIII. Rib Waveguide

The rib waveguide is another type of dielectric waveguide having considerable practical importance. This is a special type of slab-coupled waveguide, where the loading strip is made out of the same material as the slab. We have analyzed a GaAs/GaAlAs rib waveguide, where the dielectric constant of the rib and the slab is 11.8336 and that of the substrate is 11.792356, as shown in Fig. 8. For all of these rib waveguide problems, the dimension XDL of Fig. 8 is taken as 5.0 μm, and $YDL + YARM$ is taken to be constant and equal to 3.0 μm. Fig. 8 shows the propagation characteristics for the H_{11}^x mode for five different rib heights, including a point from Austin [27]. Fig. 9 shows propagation characteristics for four modes when the rib height is 0.5 μm. Fig. 10 shows the field variation in the symmetry plane normal to the surface, for different frequencies. Fig. 11(a) and (b) shows eigenvectors for H_{11}^x modes for two different rib heights.

IX. Image Lines

At millimeter and submillimeter wavelengths, the dielectric image guide is a convenient form of waveguide. The geometry of an image line, as shown in Fig. 12, consists of a rectangular dielectric slab with relative permittivity ϵ_r, backed by a perfectly conducting metal plate, and surrounded by a semi-infinite medium of lower dielectric constant (usually air). We have solved a typical structure (10.0 mm $\times$ 5.0 mm guide) with dielectric constant 1.05, and its propagation characteristics are shown in Fig. 12. In Fig. 13, we compare the solution of image lines having different dielectric constants. Fig. 14(a) and (b) shows eigenvectors for two modes of an image line. We have also solved an image line with a deformed cross section due to the fabrication process used. Its dielectric constant was unknown, but its experimental dispersion curve was available [28]. We concluded that a dielectric constant value about 7.5 is a reasonable approximation for the unknown value. Associated dispersion curves are shown in Fig. 15.

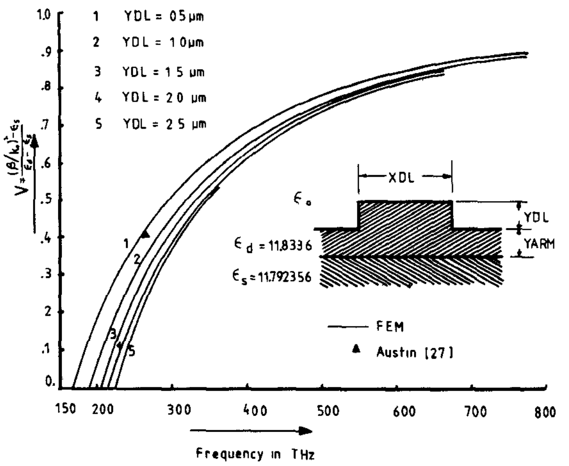

Fig. 8. Propagation characteristics for H_{11}^x modes in rib waveguides for different rib heights.

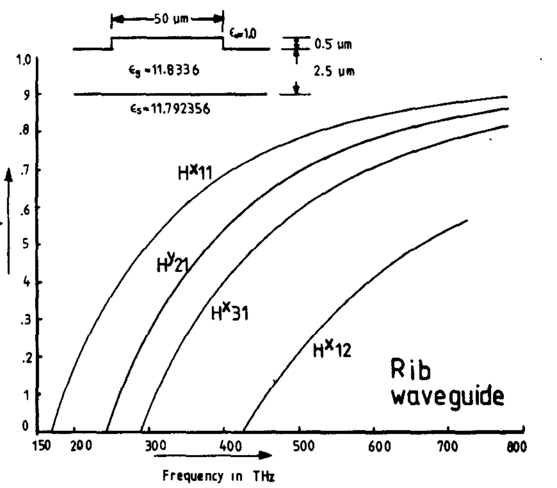

Fig. 9. Propagation characteristics for four modes in rib waveguide, $YDL = 0.5$ μm, and $YARM = 2.5$ μm.

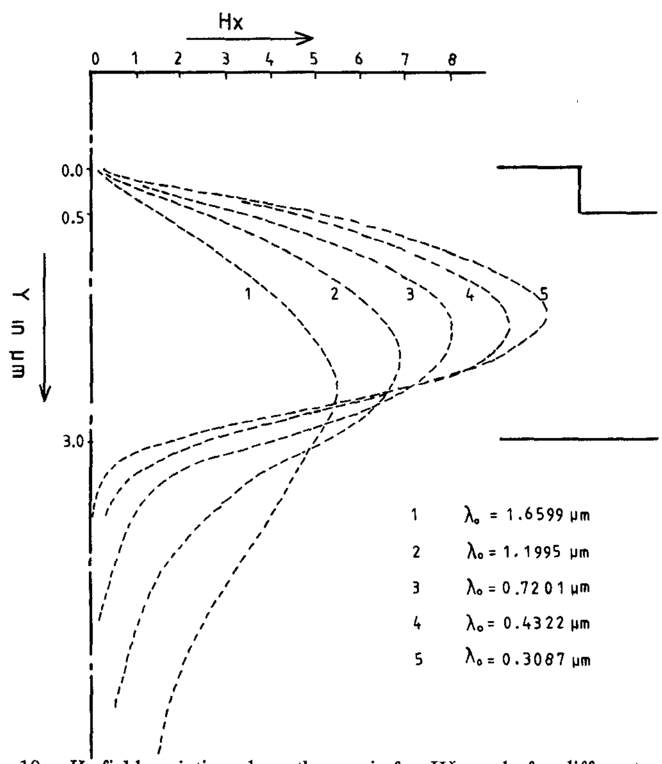

Fig. 10. H_x field variation along the y-axis for H_{11}^x mode for different frequencies $YDL = 0.5$ μm.

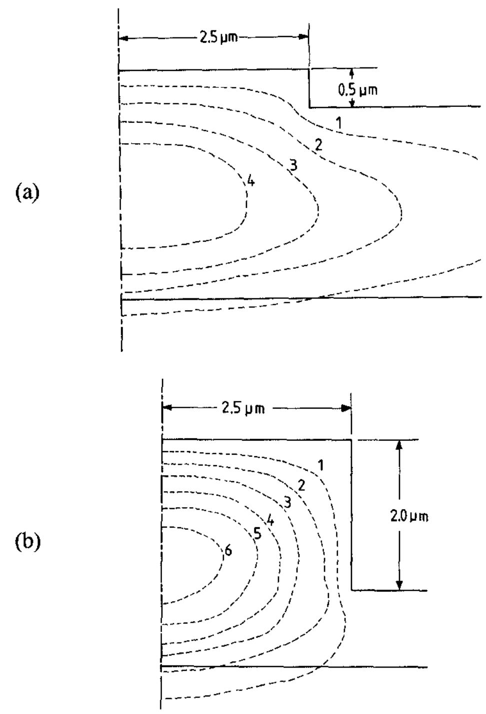

Fig. 11. H_x field contour at 0.4502-μm wavelength. (a) $YDL = 0.5$ μm. (b) $YDL = 2.0$ μm.

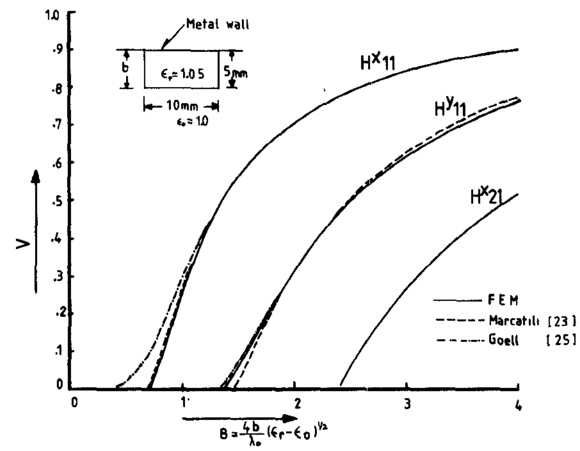

Fig. 12. Normalized propagation characteristics for an image line, mesh division 9×9.

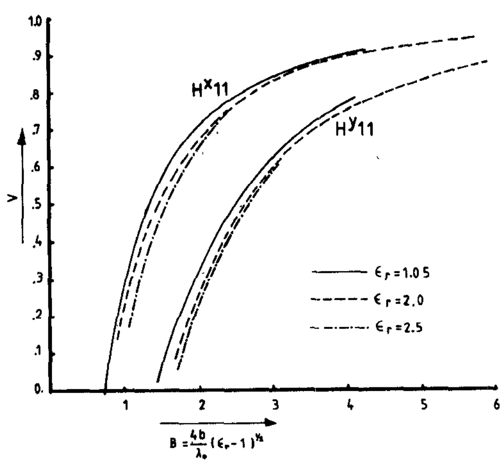

Fig. 13. Comparison of normalized propagation characteristics for image lines with different dielectric constants, mesh division 9×9.

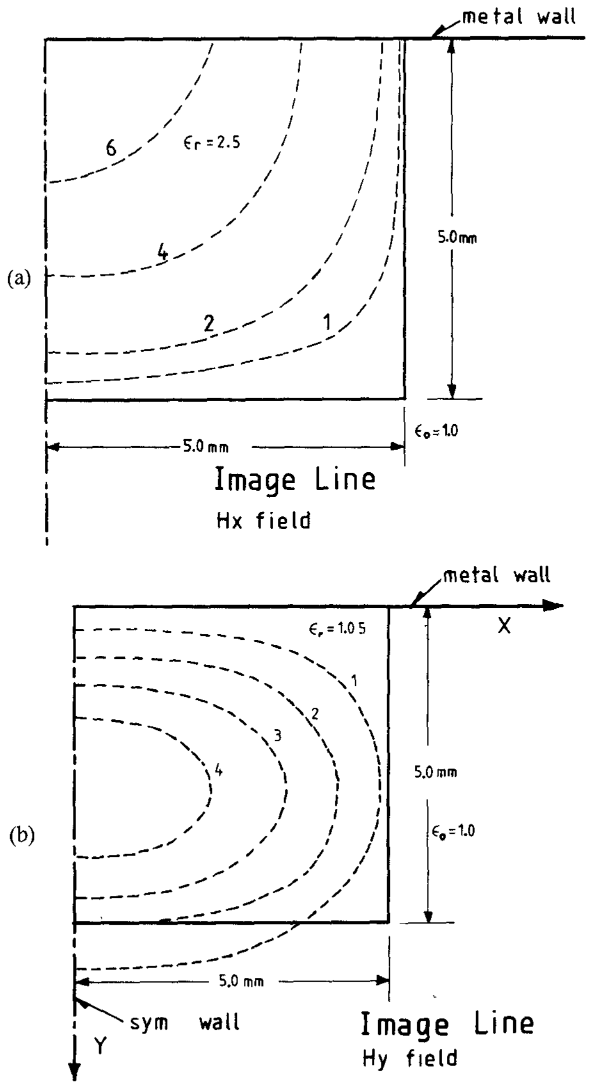

Fig. 14. Field contour for image line. (a) H_x field, $\epsilon_r = 2.50$, H_{11}^x mode. (b) H_y field, $\epsilon_r = 1.05$, H_{11}^y mode.

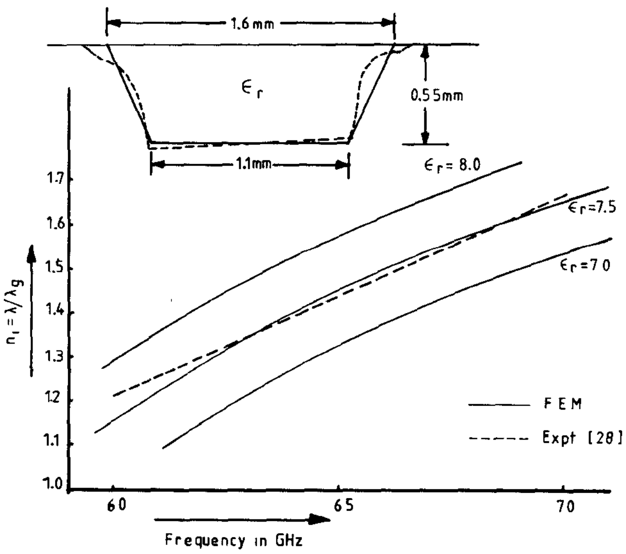

Fig. 15. Propagation characteristics for H_{11}^x mode in the trapezoidal image line, approximating the indicated experimental cross section.

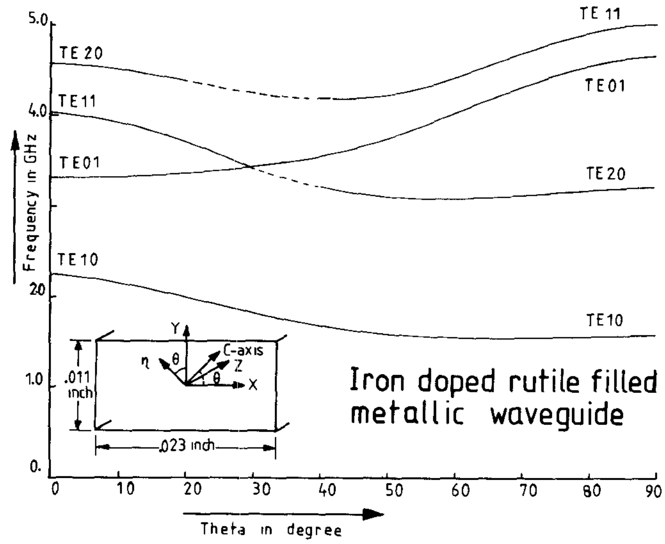

Fig. 16. Variation of cutoff frequency, with theta for four TE modes in an anisotropic waveguide, mesh division 14×14.

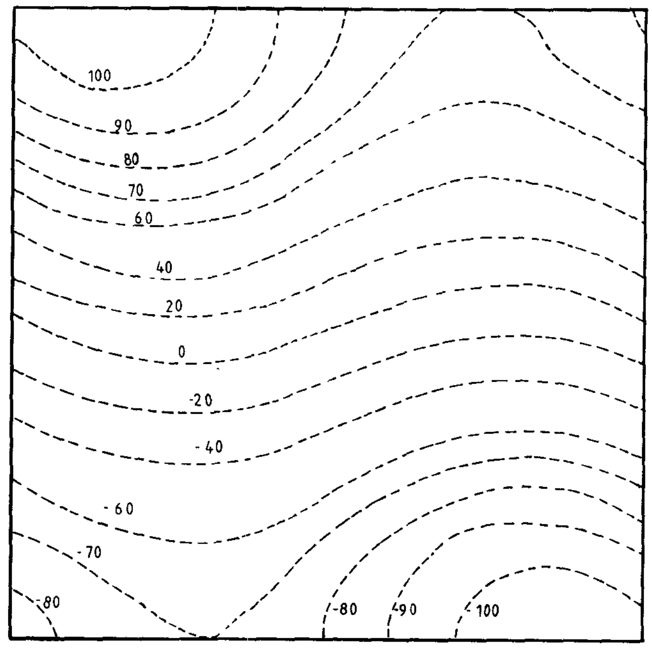

Fig. 17. H_z field contour for TE_{10} mode in anisotropic waveguide at theta = 30°.

X. Anisotropic Waveguide

A number of important applications of anisotropic media have come to the forefront in the field of electromagnetic waves. It is quite important for crystalline materials, such as $LiNbO_3$ or GaAs, as used for optical waveguides. Their special tensor properties can be exploited to design phase shifters, modulators, etc. [29]. To properly analyze these structures, we need a method which is able to handle structures with general anisotropy, and the ***H*** field FEM is capable of doing so. Here we show the results of a metallic rectangular waveguide loaded with iron-doped rutile. Its crystal *c*-axis lies in the transverse plane at any arbitrary angle θ with the larger side. The dielectric constants of this material are 260.0 along the *c*-axis, and 130.0 along the

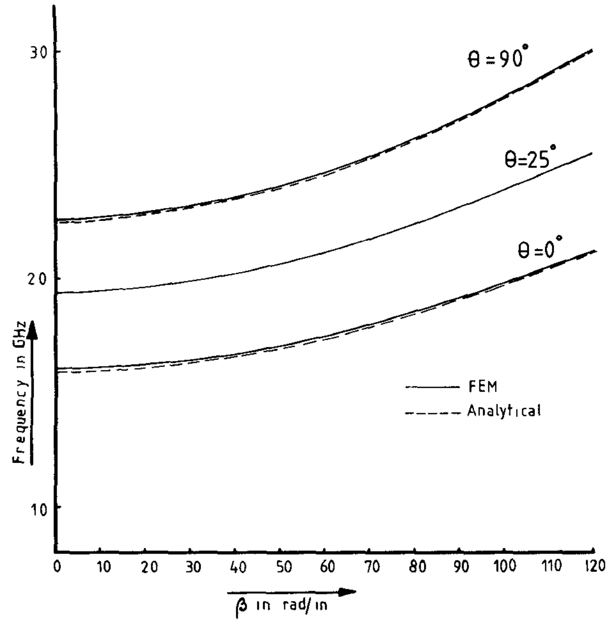

Fig. 18. Variation of frequency, with propagation constant, for a TE_{10} mode in an anisotropic waveguide, mesh division 6×6.

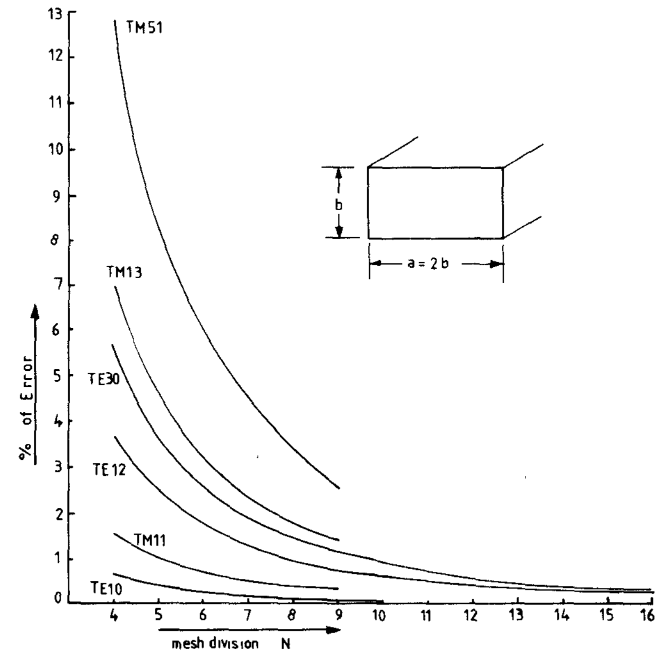

Fig. 19. Variation of percentage errors for different modes in a rectangular metallic waveguide with mesh division $N \times N$.

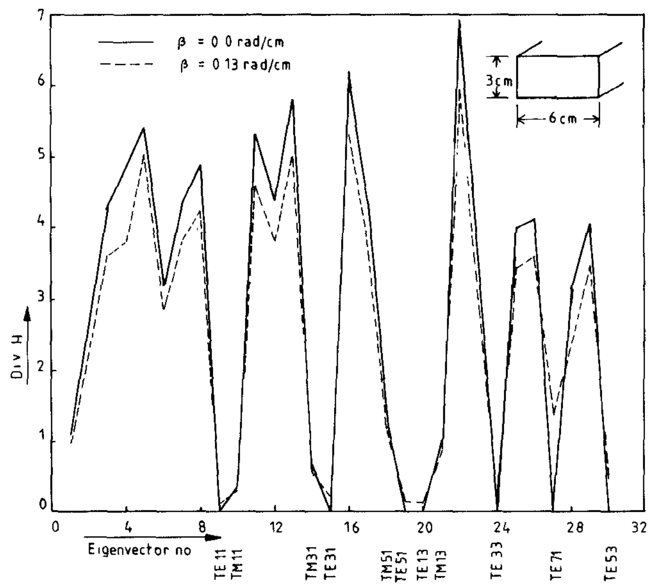

Fig. 20. Variation of divergence for a few eigenvectors in a rectangular metallic waveguide.

transverse axes. The fully loaded guide's dimension is taken to be 0.023 in × 0.011 in, as in [30]. Its variation of the cutoff frequency for different modes with different θ's is given in Fig. 16. We plot the H_z field contours for the TE_{10} mode in Fig. 17. We show the accuracy of the FEM method compared to an analytical method (which is possible only for $\theta = 0°$ or 90°), and the variation of frequency with the propagation constant in Fig. 18.

XI. Computational Remarks

We have solved a wide range of waveguide propagation problems using a vector finite-element method. In the finite-element method, one needs quite a large number of elements or nodal points to achieve satisfactory accuracy of the solution. Error in the solution decreases as the mesh number increases, as the numerical model comes closer to the continuous physical problem. This is shown in Fig. 19. We can increase the accuracy by using a higher number of elements, or by using higher order shape functions, or by using extra-precision word length.

Mention was made in Section V of the appearance of "spurious" modes in addition to the true physical modes. We have identified the spurious solutions from the true solutions by using the "divergence test" [2], where we calculate $|\text{div}\boldsymbol{H}|$ of each possible mode from the computed nodal field values, and then integrate and compare them. A true eigenvector invariably has a smaller value of $|\text{div}\boldsymbol{H}|$ than a spurious one. Fig. 20 shows $|\text{div}\boldsymbol{H}|$ for a few modes for an empty rectangular metallic waveguide.

For most of our problems, we have divided the structure domain into 100 to 200 triangles, and corresponding matrices' orders were around 150 to 350. We store *only* the nonzero elements of the highly sparse matrices, in linear arrays, and solve by using the "subspace iteration method" [2], using single-precision arithmetic. The time required by our GEC minicomputer 4082 or 4090 is around 150 to 600 i.e.u., which corresponds, roughly, to 1–5 cpu seconds on the CDC 7600 (with the FTN compiler, opt = 2).

XII. Conclusions

We present here a few of the results carried out using a vector finite-element method in conjunction with infinite elements [31]. It is found to be a powerful method to solve a wide variety of dielectric waveguide problems with anisotropic materials and unbounded regions. It is possible to use this formulation for the design of directional couplers, filters, phase shifters, modulators, etc. In this paper and earlier work [31], we have ascertained the accuracy, generality, and diversity of this formulation.

Acknowledgment

One of the authors, B. M. A. Rahman, would like to thank the Commonwealth Scholarship Commission for supporting his tenure during the research work.

References

[1] A. D. Berk, "Variational principles for electromagnetic resonators and waveguides," *IRE Trans. Antennas Propagat.*, vol. AP-4, pp. 104–111, Apr. 1956.
[2] J. B. Davies, F. A. Fernandez, and G. Y. Philippou, "Finite element analysis of all modes in cavities with circular symmetry," *IEEE Trans. Microwave Theory Tech.*, vol. MTT-30, pp. 1975–1980, Nov. 1982.
[3] S. Ahmed, "Finite element method for waveguide problems," *Electron Lett.*, vol. 4, pp. 387–389, Sept. 6, 1968.
[4] P. Silvester, "A general high-order finite-element waveguide analysis program," *IEEE Trans. Microwave Theory Tech.*, vol. MTT-17, pp. 204–210, Apr. 1969.
[5] S. Ahmed and P. Daly, "Finite element methods for inhomogeneous waveguides," *Proc. IEE*, vol. 116, pp. 1661–1664, Oct. 1969.
[6] Z. J. Csendes and P. Silvester, "Numerical solution of dielectric loaded waveguide: I-finite-element analysis," *IEEE Trans. Microwave Theory Tech.*, vol. MTT-18, pp. 1124–1131, Dec. 1970.
[7] P. Daly, "Hybrid-mode analysis of microstrip by finite element methods," *IEEE Trans. Microwave Theory Tech.*, vol. MTT-19, pp. 19–25, Jan. 1971.
[8] M. Ikeuchi, H. Sawami, and H. Niki, "Analysis of open-type dielectric waveguides by the finite-element iterative method," *IEEE Trans. Microwave Theory Tech.*, vol. MTT-29, pp. 234–239, Mar. 1981.
[9] N. Mabaya, P. E. Lagasse, and P. Vandenbuleke, "Finite element analysis of optical waveguides," *IEEE Trans. Microwave Theory Tech.*, vol. MTT-29, pp. 600–605, June 1981.
[10] K. Morishita and N. Kumagai, "Unified approach to the derivation of variational expression for electromagnetic fields," *IEEE Trans. Microwave Theory Tech.*, vol. MTT-25, pp. 34–40, Jan. 1977.
[11] W. J. English and F. J. Young, "An *E* vector variational formulation of the Maxwell equations for cylindrical waveguide problems," *IEEE Trans. Microwave Theory Tech.*, vol. MTT-19, pp. 40–46, Jan. 1971.
[12] M. Ohtaka, M. Matsuhara, and N. Kumagai, "Analysis of the guided modes in slab-coupled waveguides using a variational method," *IEEE J. Quantum Electron*, vol. QE-12, pp. 378–382, July 1976.
[13] A. Konrad, "Vector variational formulation of electromagnetic fields in anisotropic media," *IEEE Trans. Microwave Theory Tech.*, vol. MTT-24, pp. 553–559, Sept. 1976.
[14] O. C. Zienkiewicz, *The Finite Element Method*, 3rd ed. London: McGraw-Hill, 1977.
[15] K. J. Bathe and E. L. Wilson, *Numerical Methods in Finite Element Analysis*. Englewood Cliffs, NJ: Prentice Hall, 1976.
[16] F. A. F. Fernandez, "Finite element analysis of rotationally symmetric electromagnetic cavities," Ph.D. thesis, Dept. of Elec. and Elec. Eng., University College, London, 1981.
[17] P. Silvester, D. A. Lowther, C. J. Carpenter, and E. A. Wyatt, "Exterior finite elements for 2-dimensional field problems with open boundaries," *Proc. IEE*, vol. 124, pp. 1267–1270, Dec. 1977.
[18] B. H. McDonald and A. Wexler, "Finite element solution of unbounded field problems," *IEEE Trans. Microwave Theory Tech.*, vol. MTT-20, pp. 841–847, Dec. 1972.
[19] G. Mur and P. J. Fondse, "Cylindrical inhomogeneity in a homogeneous medium of infinite extent," *Microwave Opt. Acoustics*, vol. 3, pp. 224–230, Nov. 1979.
[20] C. Yeh, K. Ha, S. B. Dong, and W. P. Brown, "Single-mode optical waveguides," *Appl. Opt.*, vol. 18, pp. 1490–1504, May 1979.
[21] P. Bettes, "Infinite elements," *Int. J. Num. Meth. Eng.*, vol. 11, no. 1, pp. 53–64, 1977.
[22] D. S. Jones, *The Theory of Electromagnetism*. Oxford: Pergamon Press, 1964.
[23] E. A. J. Marcatili, "Dielectric rectangular waveguide and directional coupler for integrated optics," *Bell Syst. Tech. J.*, vol. 48, pp. 2079–2102, Sept. 1969.
[24] J. R. Winkler and J. B. Davies, "Elimination of spurious modes in finite element analysis," to be published.
[25] J. E. Goell, "A circular-harmonic computer analysis of rectangular dielectric waveguides," *Bell Sys. Tech. J.*, vol. 48, pp. 2133–2160, Sept. 1969.
[26] J. Wilkinson, Dept. of Elec. and Elec. Eng., University College, London, private communication.
[27] M. W. Austin, British Telecom Research Lab., Ipswich, England, private communication and "GaAs/GaAlAs curved rib waveguide," *IEEE Trans. Microwave Theory Tech.*, vol. MTT-30, pp. 641–646, Apr. 1982.
[28] R. V. Gelthrope, Electrical Research Association Ltd., Leatherhead, Surrey, England, private communication.
[29] R. C. Alferness, "Waveguide electrooptic modulators," *IEEE Trans. Microwave Theory Tech.*, vol. MTT-30, pp. 1121–1137, Aug. 1982.
[30] J. B. Davies, "Propagation in rectangular waveguide filled with skew uniaxial dielectric," *IEEE Trans. Microwave Theory Tech.*, vol. MTT-15, pp. 372–376, June 1967.
[31] B. M. A. Rahman, "Finite element solution of optical and microwave guides," Ph.D. thesis, Dept. of Elec. and Elec. Eng., University College, London, Oct. 1982.

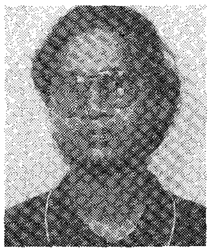

B. M. Azizur Rahman (S'80–M'83) was born in Bangladesh in 1953. He received the B.Sc. and M.Sc. degrees in electrical engineering from Bangladesh University of Engineering and Technology (BUET), Dacca, in 1976 and 1979, respectively. He received his Ph.D. degree in electronic engineering from University College, London in 1982.

From 1976 to 1979, he worked at the Electrical Engineering Department, BUET, as a lecturer. In 1983, he joined the Electrical and Electronic Engineering Department of University College, London, as an Associate Research Assistant. He worked mainly on the application of finite element technique to the solution of microwave and optical waveguide problems. His current interest is also in the solution of microstrip discontinuity problems, using the least-square boundary residual method.

J. Brian Davies (M'73) was born in Liverpool, England, in 1932. From Jesus College, Cambridge, England, he received a degree in mathematics in 1955. From the University of London, England, he received that M.Sc. degree in mathematics, the Ph.D. degree in mathematical physics, and the D.Sc. (Eng.) degree in engineering in 1957, 1960, and 1980, respectively.

From 1955 to 1963, he worked at the Mullard Research Laboratories, Salford, Surrey, England, except for two years spent at University College, London, England. In 1963, he joined the Staff of the Department of Electrical Engineering, University of Sheffield, England. Since 1967, he has been on the Staff at University College, London, where he is a Reader in Electrical Engineering. From 1971 to 1972, he was a Visiting Scientist at the National Bureau of Standards, Boulder, CO. In 1983, he was a Visitor at the Department of Engineering Science, University of Oxford, England. His research interests have been with problems of electromagnetic theory, especially those requiring computer methods of solution. But recently, his interests have extended into the field problems of acoustic microscopy and of surface acoustic waves.

Dr. Davies is a Member of the Institute of Electrical Engineers, London, England.